

ARTICLE

Open Access

Non-coding RNA dysregulation in the amygdala region of schizophrenia patients contributes to the pathogenesis of the disease

Yichuan Liu¹, Xiao Chang¹, Chang-Gyu Hahn², Raquel E. Gur³, Patrick A. M. Sleiman^{1,4} and Hakon Hakonarson^{1,4}

Abstract

Schizophrenia (SCZ) is a neuropsychiatric disorder with a complex genetic etiology. The redundancy of the gene networks underlying SCZ indicates that many gene combinations have the potential to cause a system dysfunction that can manifest as SCZ or a related neurodevelopmental disorder. Recent studies show that small non-coding microRNA (miRNA) and long non-coding RNA (lncRNA) are important factors in shaping these networks and are dynamically regulated by neuronal activation. We investigated the genome-wide transcription profiles of 46 human amygdala samples obtained from 22 SCZ patients and 24 healthy controls. Using RNA sequencing (RNA-seq), we determined lncRNA expression levels in all samples and generated miRNA profiles for 27 individuals (13 cases and 14 controls). Previous studies have identified differentially expressed miRNAs in SCZ, including miR-132, miR-212, and miR-34a/miR-34c. Here we report differential expression of a novel miRNA, miR1307, in SCZ. Notably, miR1307 maps to a locus previously associated with SCZ through GWAS. Additionally, one lncRNA that was overexpressed in SCZ, AC005009.2, also maps to a region previously associated with SCZ based on GWAS and overlapped SCZ-related genes. The results were replicated in a large independent data set of 254 dorsolateral prefrontal cortex samples from the CommonMind consortium. Taken together, these results suggest that miRNA and lncRNAs are important contributors to the pathogenesis of SCZ.

Introduction

Schizophrenia (SCZ) is a chronic, severe disabling neurodevelopmental disorder that affects people worldwide. While the exact cause of the disorder remains unknown, it is believed to result from an interplay between genetic and environmental factors^{1, 2}. Recent genetic studies have implicated multiple genomic variants in functional gene networks that individually confer modest risk to the disease rather than high-impact

mutations in single genes with large effect sizes^{3–6}. Maintaining optimal network homeostasis requires coordination by an elaborate intracellular network of molecular signal transduction systems, including microRNAs (miRNAs), which are involved in the regulation and expression of genetic networks. Therefore, in addition to gene-specific variants that may affect an individual gene or pathway manifesting as SCZ or a related neurodevelopmental disorder^{7, 8}, miRNAs such as non-coding RNAs that have the potential to dysregulate larger networks of genes have been postulated to be causal factors in the pathogenesis of SCZ⁹. Two groups of miRNAs, including typical non-coding RNAs and long non-coding RNAs (lncRNAs), have been reported to be associated with SCZ as well as other psychiatric diseases^{7,10, 11}.

Correspondence: Patrick A. M. Sleiman (sleimanp@email.chop.edu) or Hakon Hakonarson (hakonarson@email.chop.edu)

¹Center for Applied Genomics, The Children's Hospital of Philadelphia, Philadelphia, PA, USA

²Neuropsychiatric Signaling Program, Department of Psychiatry, Perelman School of Medicine, University of Pennsylvania, Philadelphia, PA, USA

Full list of author information is available at the end of the article

© The Author(s) 2018



Open Access This article is licensed under a Creative Commons Attribution 4.0 International License, which permits use, sharing, adaptation, distribution and reproduction in any medium or format, as long as you give appropriate credit to the original author(s) and the source, provide a link to the Creative Commons license, and indicate if changes were made. The images or other third party material in this article are included in the article's Creative Commons license, unless indicated otherwise in a credit line to the material. If material is not included in the article's Creative Commons license and your intended use is not permitted by statutory regulation or exceeds the permitted use, you will need to obtain permission directly from the copyright holder. To view a copy of this license, visit <http://creativecommons.org/licenses/by/4.0/>.

The amygdala dysfunction has been implicated in SCZ^{12–14}; anatomically it consists of two almond-shaped groups of nuclei located deep and medially within the temporal lobes of the human brain. Functionally, the amygdala is thought to play a primary role in the processing of memory, decision-making, and emotional reactions¹⁵. Studies in mouse models involving the amygdala suggest that overexpression of miRNAs can protect the animals against anxiety-associated responses¹⁶ and controls their fear response¹⁷. Research in human subjects also implicates the amygdala region in emotion processing and recognition of facial expressions^{18–20}. To our knowledge, a genome-wide transcription study of non-coding RNAs in the amygdala of SCZ patients has not been previously reported. In this study, we used next-generation sequencing technologies, including RNA sequencing (RNA-seq) and small RNA-seq (SRNA-seq), to assess the expression levels of miRNAs and lncRNAs in postmortem tissue from 46 individuals, including 22 SCZ patients and 24 healthy controls, obtained from the Lieber Institute. Our replication set consisted of 254 dorsolateral prefrontal cortex (DLPFC) tissues obtained from the DLPFC. Data that were generated as part of the CommonMind Consortium²¹ were of European ancestry.

Materials and methods

RNA extraction and quality assessment

Total RNA including the miRNA portion from post-mortem amygdala tissue was extracted from 100 mg of pulverized tissue with all prep DNA/RNA/miRNA Universal Kit (Qiagen). The RNA portion was purified with RNeasy Mini Spin columns and on-column DNase digestion by RNase-Free DNase Set (Qiagen). Total RNA yield was determined by Qubit RNA BR Assay Kit and Qubit Fluorometer (ThermoFisher Scientific). RNA quality was assessed with high-resolution capillary electrophoresis on an Agilent Bioanalyzer 2100 (Agilent Technologies). Approximately 300 ng of total RNA was applied to an RNA 6000 Nano LabChip without prior heating. An RIN, obtained from entire Agilent electrophoretic trace with the RIN software algorithm, was used for the assessment of RNA quality (scale 1–10, with 1 being the lowest and 10 being the highest RNA quality).

Small RNA library preparation and sequencing

The Illumina TruSeq® Small RNA kit was used to generate the small RNA-seq libraries according to the manufacturers' instructions. Briefly, 3' (RA3) and 5' (RA5) adapters were sequentially ligated to Dicer-processed miRNAs. Adaptor-ligated small RNAs were reverse-transcribed and the resultant cDNAs PCR-amplified. The PCR products were size-separated on 2% agarose gels and the 22–30 nucleotide bands excised and purified. Purified products were quantified by qPCR before cluster

generation on a cBot (Illumina). Twelve samples were multiplexed per lane and sequenced on an Illumina HiSeq2000 at 1 × 36 or 1 × 50 bp.

mRNA library preparation and sequencing

RNA-seq libraries were constructed using Illumina TruSeq RNA sample Prep Kit (RS-122-2001) TruSeq RNA Sample Prep Kit V2, Illumina Inc., San Diego, CA, 92122) following the manufacturers' instructions. The poly-A containing mRNA molecules were purified from 300 to 500 ng DNase-treated total RNA using oligo (dT) beads. Following the purification, the mRNA was fragmented using divalent cations under elevated temperature (94 degree) for 2 min. Under these conditions, the resultant fragment lengths ranged from 130 to 290 bp with a median length of 185 bp. Reverse transcriptase and random primers were used to generate the first-strand cDNA from the RNA fragments. Second-strand DNA was synthesized using DNA polymerase I and RNaseH. The resulting cDNAs were end-repaired using T4 DNA polymerase, T4 PNK, and Klenow DNA polymerase and a single "A" base added using Klenowexo (3'–5' exo minus). Illumina PE adapters were ligated using T4 DNA ligase including a barcoding index for multiplexing. These products were then purified and enriched by PCR to create the final cDNA library for high-throughput sequencing on a HighSeq2000. The concentration of the RNA-seq libraries was determined by Qubit (Invitrogen, CA) and qPCR, and the quality of the libraries assayed on a Lab ChipGX (Caliper, MA) HT DNA 1 K/12 K/Hi-sensitivity LabChip. The libraries were multiplexed and loaded on a flow cell for cluster generation on a cBot (Illumina). Illumina Real Time Analysis was used for image analysis and base calling. FASTQ files were generated using the BCL Converter (CASAVA v1.8.2).

RNA-seq/small RNA-seq alignment and differential expression test

Following sequencing we obtained an average read depth of 116 M reads per sample, ranging from 34 to 226 M reads across the 46 amygdala samples. Alignments were generated using the Genomic Short-read Nucleotide Alignment Program²² taking common SNPs (dbSNP137) into account during the alignments. The output SAM files were converted to BAM, sorted by index, and unpaired reads were filtered with SAMtools²³. Following alignment and filtering an average of 103 M reads were obtained per sample with an average mapping/filtering rate of 89% (Supplementary Table 1). Differential expression tests were performed using the *cuffdiff* package in cufflink2.2.1²⁴ and the GTF file from GENCODE version 19²⁵. The DLPFC RNA-seq data were processed using the same bioinformatics pipeline as previously described for the amygdala data. To reduce algorithm-specific false-

positives and to adjust for clinical covariates, we also analyzed the data set using DESeq2 including age, gender, postmortem index (PMI), and manner of death as covariates in the model. Differentially expressed non-coding RNAs were identified from the intersect of the Cuffdiff and DESeq2²⁶ data sets.

The small RNA-seq data read depths ranged from 4.7 to 72 M with average 20 M reads per sample. Cutadapt1.8.1 was applied to trim the adaptors²⁷ and the trimmed data were further aligned with Micro Read Fast Alignment Search Tool (MRFast)²⁸. The average mapping rate after trimming was 75.1% with an average read depth of 16 M reads per sample.

Clinical sample selection and sample data QC

A detailed description of the clinical sample is provided in Supplementary Table 6. RNA-seq and small RNA data were generated on all 49 individuals listed in Supplementary Table 6. Following primary analysis of the RNA-seq data, three individuals (10451, 10678, and 10495) were excluded from further analysis because of outlying expression values. The five most highly differentially expressed genes (*CCL3*, *CCL4*, *CCL8*, *CXCL10*, and *CXCL11*) in the analysis were driven by these three controls, with extreme fragments per kilobase million (FPKM) values ($\sim \times 100$ higher than the other samples). The outliers may be related to the cause of death of these individuals, two (10451, 10678) died from “complications of smoke inhalation”, and the third (10495) from an accident with multiple head injuries. Of the remaining 46 cases and controls, all were of Caucasian ancestry, 40 were males, and 6 females. Average age at death was 38.4 years. As confounders are an important consideration in post-mortem studies, we carried out non-parametric analyses to test for association between age, sex, and PMI with SCZ and gene expression level (FPKM) in the remaining 46 samples. No significant associations were found between FPKM or SCZ and the covariates. Following quality control of the small RNA-seq data, 19 of the 46 individuals with RNA-seq data were excluded from the analysis.

In validation data set DLPFC, RNA was isolated from 50 mg homogenized tissue in Trizol using the RNeasy kit based on the instructional protocol. The mean total RNA yield was 15.3 μg (± 5.7). The RNA integrity number (RIN) was determined by fractionating RNA samples on the 6000 Nano chip (Agilent Technologies) on the Agilent 2100 Bioanalyzer. The mean RIN was 7.7 (± 0.9), and the mean ratio of 260/280 was 2.0 (± 0.02). Processing order was re-randomized prior to ribosomal RNA (rRNA) depletion. Briefly, rRNA was depleted from about 1 μg of total RNA using Ribo-Zero Magnetic Gold kit (Illumina/Epicerter Cat # MRZG12324) to enrich for polyadenylated coding RNA and non-coding RNA. The

sequencing library was prepared using the TruSeq RNA Sample Preparation Kit v2 (RS-122–2001–48 reactions) in batches of 24 samples. A pool of 10 barcoded libraries was layered on a random selection of two of the eight lanes of the Illumina flow cell bridge amplified to ~ 250 million raw clusters. One-hundred base pair paired end reads were obtained on a HiSeq 2500. The sequence data were processed for primary analysis to generate QC values. Samples with a minimum of 50 million mapped reads (~ 25 million paired end reads) and less than 5% rRNA-aligned reads were retained for downstream analysis²¹.

Results

Replication of known SCZ-related miRNA from the small RNA-seq data

The small RNA-seq data set included 27 individuals (13 cases and 14 controls); differential expression analysis resulted in the identification of 17 statistically significant differentially expressed miRNAs (Table 1). Ten of the seventeen are novel discoveries, the remaining seven have previously been implicated in SCZ and/or other psychiatric phenotypes, including two members of miRNA family 34, mir-34c, -34a (p value = $3e-4$ and 0.02, respectively) as well as a number of others including mirs-124, -132, -212, -663, and -144.

miRNA based on RNA-seq

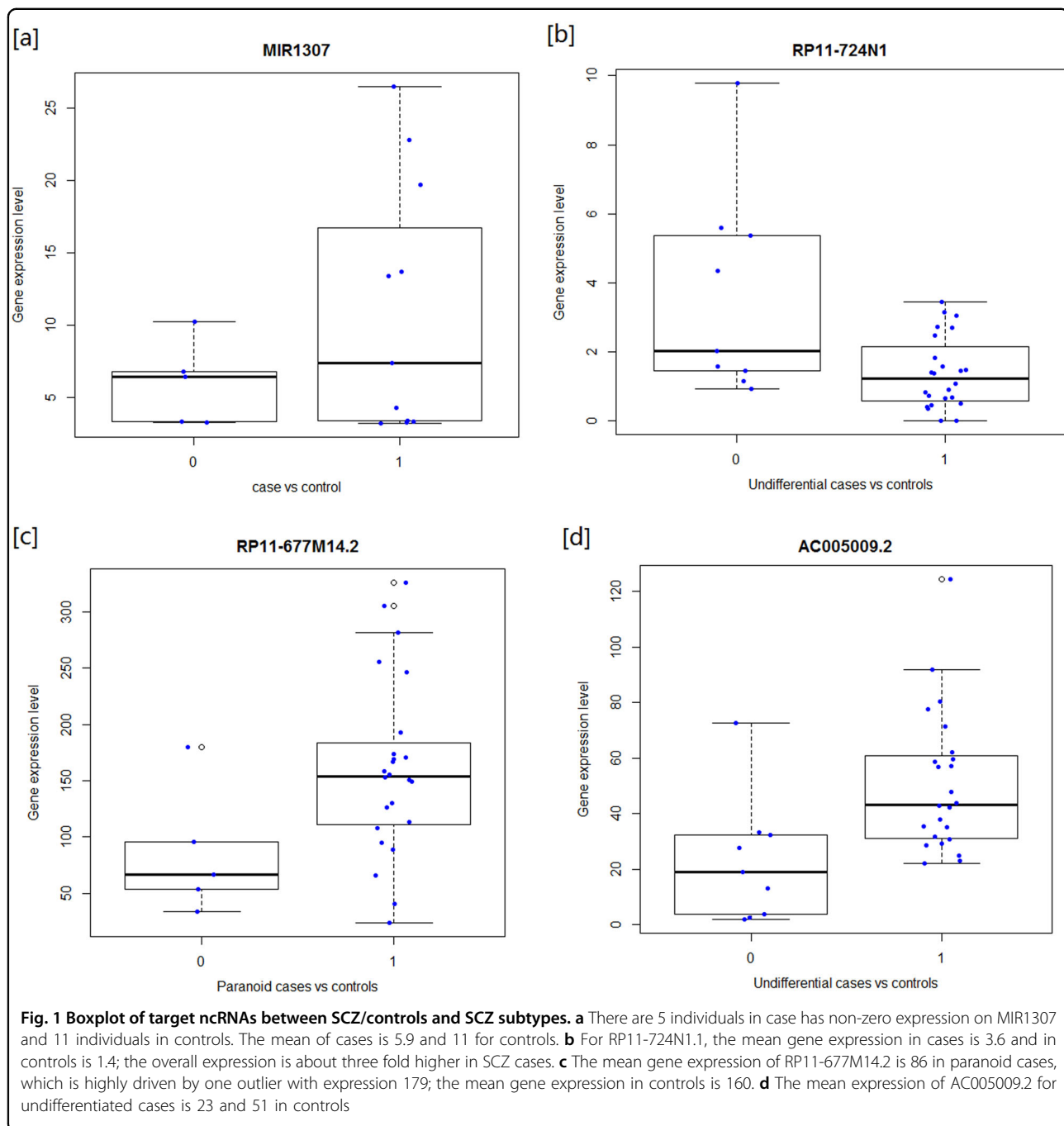
While RNA-seq is not designed to systematically detect expression changes of miRNA, some miRNAs that are affiliated with the RNA class are detectable by RNA-seq. Analysis of the GTF file as described in the Materials and methods section resulted in the identification of differential expression of *MIR1307* between the SCZ patients and healthy controls. Expression of *MIR1307* was approximately threefold higher in controls (p value = 0.0152). The expression difference and the direction of change were confirmed in the small RNA-seq data set, plotting the expression levels in cases and controls confirms that the association is not driven by outliers (Fig. 1a).

LncRNAs based on RNA-seq

Differential analysis of the transcriptome data identified 250 lncRNAs from Gencode version 19 that showed significant expression differences between the amygdala regions of cases and controls (Supplementary Table 2). Among those, two lncRNAs *RP11-724N1.1* (p value = 0.014) and *RP11-677M14.2* (p value = 0.045) are of particular interest as they map to regions previously associated with SCZ based on genome-wide association study (GWAS) (Table 2). *RP11-724N1.1* resides within the GWAS locus on chr10, previously shown to be associated with SCZ in multiple studies^{29, 30}. *RP11-677M14.2* is located within the SCZ-associated gene, neurogranin

Table 1 MicroRNA differentially expressed based on small RNA-seq of 27 individuals

MicroRNA_ID	Locus	FPKM_SCZ	FPKM_controls	p value	Previous SCZ miRNA	Functions
hsa-mir-196a-2	chr12:54385521-54385631	90.3847	0	5.00E-05	N	
hsa-mir-1975	chr7:148638579-148638654	6.93E+06	3.38E+06	0.00015	N	
hsa-mir-663	chr20:26188821-26188914	1352.72	3820.51	0.00015	Y	Suppresses the expression of multiple genes implicated in neurogenesis
hsa-mir-34c	chr11:111384163-111384240	777.765	346.426	0.0003	Y	Acute restraint stress in rodents were observed in the central amygdala, increasing expression of hsa-mir-34c introduce to anxiety
hsa-mir-639	chr19:14640354-14640452	5.59116	87.504	0.0007	N	
hsa-mir-132	chr17:1953201-1953302	1.40E+06	2.12E+06	0.00235	Y	Bipolar in mouse; gene network in MDD patients; differentially expressed in human prefrontal cortex; potential biomarker for SCZ
hsa-mir-124-2	chr8:65291705-65291814	1046.85	2008.49	0.00655	Y	Link to anxiety through glucocorticoid signaling
hsa-mir-451	chr17:27188386-27188458	6.95E+06	4.97E+06	0.01085	N	
hsa-mir-212	chr17:1953564-1953674	58.2733	91832	0.0125	Y	Differentially expressed in human prefrontal cortex; potential biomarker for SCZ
hsa-mir-483	chr11:2155363-2155439	2268.02	5351.61	0.01525	N	
hsa-mir-886	chr5:135416176-135416297	2773.91	5943.91	0.0226	N	
hsa-mir-34a	chr1:9211726-9211836	45.6068	30.7747	0.0234	Y	Control fear response in mice amygdala; differentially expressed in human prefrontal cortex. Potential biomarkers in blood for SCZ
hsa-mir-375	chr22:19866366-219866430	47.4196	25.4854	0.02615	N	
hsa-mir-585	chr5:168690604-168690698	3850.95	6422.48	0.03325	N	
hsa-mir-424	chrX:133680643-133680741	16.779	25.251.9	0.038	N	
hsa-mir-144	chr17:27188550-27188636	229.142	160.058	0.04165	Y	Dysregulated in hippocampus of rats by the mood stabilizers valproate and lithium
hsa-mir-520d	chr19:54223349-54223436	18.5836	89.2044	0.0489	N	



(NRGN)³⁰, the human homolog of the neuron-specific rat RC3/neurogranin gene, which is a direct target for thyroid hormone in the human brain, and controls its expression.

Non-coding RNAs for SCZ subtypes

We further categorized the SCZ patients based on their clinical subtypes, including disorganized (seven individuals), paranoid (five individuals), and undifferentiated (nine individuals; Supplementary Table 7). The analysis revealed subtype specificity in non-coding RNA

expression levels. MIR1307 showed 10-fold higher expression in controls when compared with the undifferentiated subtype in contrast to a two-fold increase when compared with the paranoid subtype. MIR1282 showed significantly higher expression in the paranoid subtype. We also identified subtype specificity in the expression of miRNAs previously reported to be associated with SCZ or other psychiatric diseases. For instance, the miRNA family 34 were only significant in the undifferentiated subtype and mir-144 was only associated

Table 2 Summary of lncRNAs associated with SCZ

LncRNA	RP11-724N1.1	RP11-677M14.2
Locus	chr10:104674341–104675161	chr11:124614529–124616233
FPKM_SCZ	2.6918	110.377
FPKM_control	1.41326	148.519
<i>p</i> value	0.014	0.04545
SCZ GWAS regions	chr10:104487871–105245420, chr10:104423800–105165583,	chr11:124610007–124620147,
SCZ SNPs	rs2297787 (<i>p</i> value = 1.53E–13; distance = 4976 bp), rs11191419 (<i>p</i> value = 9.24E–18; distance = 62k bp), rs55833108 (<i>p</i> value = 1.42E–8; distance = 66k bp)	rs55661361 (<i>p</i> = 3.68E–12; distance = 578 bp)
Nearby genes	CNNM2	NRGN

Table 3 Replications of target lncRNAs/miRNA in dorsolateral prefrontal cortex tissues (DLPFC)

Tissue	LncRNA	Locus	Case	Control	<i>pV</i>
Amygdala	RP11-724N1.1	chr10:104674341–104675161	3.57426	1.37889	0.01605
DLPFC	RP11-724N1.1	chr10:104674341–104675161	1.81873	1.65285	NA (no enough reads)
Amygdala	RP11-677M14.2	chr11:124614529–124616233	85.7424	160.158	0.0064
DLPFC	RP11-677M14.2	chr11:124614529–124616233	4.01757	4.47271	0.27675
Amygdala	AC005009.2	chr7:86413541–86415986	22.9313	50.602	0.00165
DLPFC	AC005009.2	chr7:86413541–86415986	69.0017	92.058	0.0006
Amygdala	mir1307	chr10:105154009–105154158	1.36	4.08	0.0152
DLPFC	mir1307	chr10:105154009–105154158	5.16	8.18	NA (no enough reads)

with the disorganized subtype (Supplementary Table 4). For lncRNAs, *RP11-677M14.2* was shown to be differentially expressed in the paranoid subtype (*p* value = 0.0064), whereas *RP11-724N1.1* was differentially expressed in undifferentiated SCZ (*p* value = 0.016; Supplementary Table 5). Finally, some associations were restricted to a particular subtype such as lncRNA *AC005009.2*, which was not differentially expressed in the combined analysis but is significantly associated with the undifferentiated subtype (*p* value 0.0016).

Plotting the expression value distributions of the three lncRNAs differentially expressed by subtype (Supplementary Figs. 2a–e) indicates that the results are not driven by outliers. To determine the effects of variables such as age, gender, and manner of death (Supplementary Fig. 3), we used expression values of target lncRNAs as dependent variable (*y*) and age, gender, and mode of death as independent variable (*x*). For *RP11-724N1.1*, the *p* value of linear regression is 0.312, 0.973, and 0.504 for age of death, gender, and manner of death. For *RP11-677M14.2* the *p* values are 0.2735, 0.3565, and 0.0954, and for *AC005009.2* the *p* values are 0.0429, 0.7158, and 0.7331, respectively. Therefore, the expression level

differences of subtypes are not driven by the biological parameters at a significance level of $p \leq 0.01$. The entire distribution difference *p* values of expressed lncRNAs based on Wilcoxon rank-sum between undifferentiated, paranoid, and disorganized are 0.056, 0.15, and 0.89. The statistic results indicate that the lncRNA distribution between undifferentiated and paranoid are close to significant difference, and there are certain level differences between paranoid and disorganized, but the differences between undifferentiated and disorganized are insignificant. As a result, it suggests that paranoid SCZ has unique lncRNA patterns compared to other subtypes.

The DESeq2 results of the three lncRNAs were highly concordant with the cuffdiff outputs, expression fold changes were consistent, and almost identical between two tools (Supplementary Table 8). The boxplot of those three lncRNAs showed that the expression differences are not driven by outliers (Figs. 1b–d).

Replication/validation from independent data set

With limited availability of postmortem amygdala tissue from SCZ patients and no previously reported human amygdala RNA-seq studies available in the public domain,

we attempted replication of our findings in DLPFC²¹, an independent data set from the CommonMind Consortium. RNA-seq was carried out in the DLPFC of totally 254 individuals (120 SCZ and 134 controls) of European ancestry. We applied the same bioinformatics analysis pipeline to the DLPFC data as previously described for the amygdala data to validate our lncRNA/miRNA findings. Adequate coverage was obtained for lncRNA *AC005009.2* in the replication set but not for the rest three non-coding RNAs. The read depth of DLPFC data set is about half that of the amygdala data at 60~70 M reads vs. 150 M reads. As shown in Table 3, *AC005009.2* replicated with a significant *p* value, and MIR1307 showed a clear trend toward association, with the same direction of effect, in the DLPFC data (Table 3).

Discussion

SCZ is a complex polygenic disease. Multiple risk genes have already been identified through GWAS and sequencing studies^{30, 31}. To date, no variants, common or rare, conferring large effect sizes have been identified in SCZ. Rather a picture is emerging from the genetic studies implicating the dysregulation of complex gene networks and regulatory mechanisms. Growing evidence indicates that distinct neuronal ncRNAs, particularly miRNAs and lncRNAs, are likely to influence the development of psychiatric diseases, including SCZ. For instance, the lncRNA, *Gomafu*, is acutely regulated in response to neuronal activation and is involved in SCZ-associated alternative splicing. In this study, we detected altered expression of miRNAs and lncRNAs, well defined in GENCODE annotation, by RNA-seq and SRNA-seq of amygdala tissue samples from 46 subjects including SCZ subjects and controls.

Amygdala dysfunction has been extensively reported in SCZ, yet to our knowledge, gene expression profiling has not been previously reported on human amygdala tissue. Previous studies in mice show that overexpression of miRNA 34 genes in amygdala is associated with anxiety and fear. Overexpression of *mir-34c* in the amygdala of mice has been shown to induce anxiolytic behavior after challenge¹⁶; in our data set, the expression of *mir-34c* was twofold higher in the SCZ group compared to the control. *Mir-34a* has been implicated in amygdala-dependent fear memory consolidation in mice through Notch signaling¹⁷ and in our data expression of *mir-34a* was significantly upregulated in cases. *Mir-34a* has been shown to be differentially expressed in other brain regions, including the prefrontal cortex³², leading to the suggestion that *mir-34a* levels in blood could serve as a biomarker for SCZ^{33, 34}. In our study, we identify that the 34 family is only differentially expressed in the individuals with “undifferentiated” subtype of SCZ. Another example is *mir-132*, a well-known miRNA involved with circadian rhythm and

Table 4 Gene expressions of SCZ GWAS region chr10:104487871–105245420

Categories	Gene ID	<i>p</i> value
Gene in relation to index SNP	C10orf32-AS3MT	na
	C10orf26	0.59655
	CALHM1	0.3712
	CALHM2	0.5112
	CALHM3	na
	CNNM2	0.7684
	CYP17A1	na
	INA	0.14265
Other genes in genomic region defined by LD	MIR1307	0.0152
	NT5C2	0.87125
	PCGF6	0.57665
	PDCD11	0.8658
	SFXN2	0.5662
	TAF5	0.9112
	USMG5	0.98425
	ACTR1A	0.96425
	ARL3	0.6029
	AS3MT	0.80155
eQTL	C10orf26	0.59655
	C10orf32	0.41385
	NT5C2	0.87125
	TMEM180	0.6154
	TRIM8	0.5002

“na” indicates there is not enough coverage for the gene

previously associated with multiple psychiatric traits in mouse models³⁵ and with network regulation in major depressive disorder in human prefrontal cortex tissue³⁶. *Mir-132* is also differentially expressed in human prefrontal cortex tissue in miRNA-profiling data³² and is a potential biomarker in human blood³³. In our study, we show that *mir-132* is differentially expressed across all of the clinical SCZ subtypes. Another miRNA of interest, *mir-663*, is a known regulator of neuronal differentiation³⁷. Finally, *mir-144* is expressed in the hippocampus of rats and is known to be influenced by both valproate and the mood stabilizer lithium³⁸; *mir-144* is found to be only differentially expressed in individuals categorized as “disorganized” SCZ.

In addition to the seven previously reported miRNAs, we further identified 10 miRNAs that will require validation in future human or mouse studies. We also identified over 200 differentially expressed lncRNAs in this

study. In order to prioritize the lncRNAs, we focused on differentially expressed lncRNAs that mapped to previously reported GWAS loci. Two lncRNAs, *RP11-724N1.1* and *RP11-677M14.2*, mapped to GWAS loci at chr10q24.3 and chr11q24.2, respectively. *RP11-724N1.1* maps to the third most significantly associated region from the PGC2 SCZ meta-analysis (rs11191419, p value = 6.29×10^{-19})³⁹. Similar to miRNAs, *RP11-724N1* is also clinical subtype-specific; it is only differentially expressed in undifferentiated SCZ subtype. *RP11-724N1.1* overlaps the *CNNM2* gene, as shown in Supplementary Fig. 1a. *CNNM2* encodes a brain-expressed transmembrane protein that is involved in magnesium transport⁴⁰. Loss of function mutations in *CNNM2* has recently been reported to be causal of hypomagnesemia, seizures, and mental retardation⁴¹. *RP11-677M14.2* maps to the antisense strand overlapping the *NRGN* gene (Supplementary Fig. 1b). The *NRGN* locus has been shown to be associated with SCZ in the PGC2 meta-analysis (rs55661361, p value = $3.68E-12$), as well as in multiple other studies that reported association of functional coding variants in *NRGN* with SCZ^{39, 42–45}. Post-transcriptional regulation of *NRGN* through overlapping sense and antisense transcripts has previously been reported during cerebral corticogenesis and synapse function in mice⁴⁶. We can confirm through our RNA-seq expression data (Supplementary Table 3) that the expression of *NRGN* is strikingly higher (FPKM = 1251) in the SCZ group compared to controls (FPKM = 0). Subtype analysis further indicated that *RP11-677M14.2* under expression was restricted to cases with a clinical diagnosis of paranoid SCZ.

A subtype-specific lncRNA, AC005009.2, has been identified for undifferentiated SCZ individuals; the lncRNA shows twofold higher expressions in control compared to SCZ patients who were diagnosed as the “undifferentiated” subtype. AC005009.2 is also close to GWAS region of PGC2 SCZ meta-analysis (rs12704290, p value = 1.04×10^{-10}). Meanwhile, AC005009.2 overlaps the transcript of the metabotropic glutamate receptor 3 gene (*GRM3*; Supplementary Fig. 5c). *GRM3* has been shown to associate with SCZ risks in previous studies^{47–49}, and AC005009.2 is only differentially expressed in undifferentiated SCZ subtype with p value = 0.0046 and 1.5-fold higher expression in controls.

MIR1307 also maps to a highly significant SCZ GWAS locus (rs11191419, p value = $6.198e-19$) in the PGC2 meta-analysis³⁰. The associated locus contains multiple genes; however, we only detected differential expression in our RNA-seq data set from *MIR1307* (Table 4). The expression data raise the possibility that the GWAS association is being driven by *MIR1307*. Further work will be required to assess the association between the SCZ-associated GWAS variants and *MIR1307* expression levels in the brain.

To validate and replicate our findings in the absence of an independent human amygdala RNA-seq data set, we turned to a much larger independent data set of 254 prefrontal cortex tissues. The involvement of the DLPFC in SCZ is well established with multiple reports of association of DLPFC dysfunction correlating with clinical phenotype^{50, 51}. *AC005009.2* replicated with a significant p value and *MIR1307* showed a clear trend toward association, with the same direction of effect, in the DLPFC data. The two other lncRNAs, *RP11-724N1.1* and *RP11-677M14.2*, did not reach statistical significance in the DLPFC data, which may either be reflective of tissue specificity or simply due to the reduced coverage in the DLPFC data. The average read coverage in the DLPFC was 70 M reads compared with the 150 M reads from the amygdala data.

Finally, we note that several previously reported SCZ-associated miRNAs, including *MIR137*, *181b*, *19*, *219*, and *MIR9*, did not replicate in this study. *MIR137* and *MIR181b* were based on GWAS results rather than brain tissues, and *MIR181b* was reported in Chinese population rather than in Caucasian^{52–54}. GWAS studies based on blood showed that *MIR137* mediated dysregulation as a previously unknown etiologic mechanism in SCZ⁵². Our results showed that *MIR137* expression is almost same in SCZ and controls, and *MIR181b* is 1.2-fold higher than SCZ. *MIR19* was reported recently to have abnormal expression in neural progenitor cells from SCZ patient-derived induced pluripotent stem cells (iPSCs)⁵⁵; in our data the expression of *MIR19* was 1.2-fold higher in SCZ patients, but it did not reach significance (p value = 0.43). *MIR219*, a brain-specific miRNA, was reported in both normally developing and SCZ patient iPSC-derived neural stem cells⁵⁶. In our amygdala data, the expression level of *MIR219* was 1.4-fold higher in SCZ; however, it did not reach significance with a p value of 0.19. The association of those two miRNA was initially reported in SCZ NPCs but not in brain tissue, which may explain the lack of replication. *MIR-9* was reported to be abundantly expressed in control neural progenitor cells (NPCs) and significantly downregulated in a subset of SCZ NPCs⁵⁷. In Cuffdiff pipeline, the *mir-9* was marked as region with too many fragments, so no p value was generated. In contrast, DESeq2 reports significant q value of *mir-9* (0.02).

Conclusion

Differential expression analysis of small RNAs in SCZ brain identified multiple genes that may be contributing to the pathogenesis of the disease. Intersecting the list of differentially expressed small and lncRNAs with loci identified in previously reported GWAS studies has highlighted two genes, miRNA (*mir1307*) and lncRNAs (*AC005009.2*), that are differentially expressed in SCZ and as such may underlie or contribute to the observed

GWAS signals at these loci. This study demonstrates the utility of transcriptional profiling of relevant disease tissues in identifying genes underlying GWAS signals.

Acknowledgments

We thank Dr. Joel E. Kleinman, Dr. Dan R. Weinberger, and Dr. Thomas M. Hyde from The Lieber Institute for Brain Development | LIBD, Baltimore, MD for contributing the samples. DLPFC data were generated as part of the CommonMind Consortium supported by funding from Takeda Pharmaceuticals Company Limited, F. Hoffman-La Roche Ltd, and from NIH grants R01MH085542, R01MH093725, P50MH066392, P50MH080405, R01MH097276, R01MH-075916, P50M096891, P50MH084053S1, R37MH057881, and R37MH057881S1, HHSN271201300031C, AG02219, AG05138, and MH06692. Brain tissue for the study was obtained from the following brain bank collections: the Mount Sinai NIH Brain and Tissue Repository, the University of Pennsylvania Alzheimer's Disease Core Center, the University of Pittsburgh NeuroBioBank and Brain and Tissue Repositories, and the NIMH Human Brain Collection Core. CMC Leadership: Pamela Sklar, Joseph Buxbaum (Icahn School of Medicine at Mount Sinai), Bernie Devlin, David Lewis (University of Pittsburgh), Raquel Gur, Chang-Gyu Hahn (University of Pennsylvania), Keisuke Hirai, Hiroyoshi Toyoshiba (Takeda Pharmaceuticals Company Limited), Enrico Domenici, Laurent Essioux (F. Hoffman-La Roche Ltd), Lara Mangravite, Mette Peters (Sage Bionetworks), Thomas Lehner, and Barbara Lipska (NIMH).

Author details

¹Center for Applied Genomics, The Children's Hospital of Philadelphia, Philadelphia, PA, USA. ²Neuropsychiatric Signaling Program, Department of Psychiatry, Perelman School of Medicine, University of Pennsylvania, Philadelphia, PA, USA. ³Neuropsychiatry Section, Department of Psychiatry, Perelman School of Medicine, University of Pennsylvania, Philadelphia, PA, USA. ⁴Division of Human Genetics, Department of Pediatrics, The Perelman School of Medicine, University of Pennsylvania, Philadelphia, PA, USA

Ethical approval

This study had been approved by the Children's Hospital of Philadelphia with IRB# 4886. All the patients who participated in this project have been consented and they agree to publish the results.

Competing interests

The authors declare that they have no competing financial interests.

Publisher's note: Springer Nature remains neutral with regard to jurisdictional claims in published maps and institutional affiliations.

Supplementary information

The online version of this article (<https://doi.org/10.1038/s41398-017-0030-5>) contains supplementary material.

Received: 21 June 2017 Accepted: 20 August 2017

Published online: 02 February 2018

References

- Picchioni, M. M. & Murray, R. M. Schizophrenia. *Br. Med. J.* **335**, 91–95 (2007).
- van Os, J. & Kapur, S. Schizophrenia. *Lancet* **374**, 635–645 (2009).
- Harrison, P. J. & Weinberger, D. R. Schizophrenia genes, gene expression, and neuropathology: on the matter of their convergence. *Mol. Psychiatry* **10**, 40–68 (2005). image 45.
- Sun, J. et al. Schizophrenia gene networks and pathways and their applications for novel candidate gene selection. *PLoS ONE* **5**, e11351 (2010).
- Talkowski, M. E. et al. A network of dopaminergic gene variations implicated as risk factors for schizophrenia. *Hum. Mol. Genet.* **17**, 747–758 (2008).
- O'Donovan, M. C., Craddock, N. J. & Owen, M. J. Genetics of psychosis; insights from views across the genome. *Hum. Genet.* **126**, 3–12 (2009).
- Beveridge, N. J. & Cairns, M. J. MicroRNA dysregulation in schizophrenia. *Neurobiol. Dis.* **46**, 263–271 (2012).
- Mericò, D. et al. MicroRNA dysregulation, gene networks, and risk for schizophrenia in 22q11.2 deletion syndrome. *Front. Neurol.* **5**, 238 (2014).
- Mamdani, F. et al. Coding and noncoding gene expression biomarkers in mood disorders and schizophrenia. *Dis. Markers* **35**, 11–21 (2013).
- Kocerha, J., Dwivedi, Y., Brennand, K. J. Noncoding RNAs and neurobehavioral mechanisms in psychiatric disease. *Mol. Psychiatry* **20**, 677–684 (2015).
- Barry, G. et al. The long non-coding RNA Gomafu is acutely regulated in response to neuronal activation and involved in schizophrenia-associated alternative splicing. *Mol. Psychiatry* **19**, 486–494 (2014).
- Lawrie, S. M., Whalley, H. C., Job, D. E. & Johnstone, E. C. Structural and functional abnormalities of the amygdala in schizophrenia. *Ann. N. Y. Acad. Sci.* **985**, 445–460 (2003).
- Mahon, P. B. et al. An MRI study of amygdala in schizophrenia and psychotic bipolar disorder. *Schizophr. Res.* **138**, 188–191 (2012).
- Rasetti, R. et al. Evidence that altered amygdala activity in schizophrenia is related to clinical state and not genetic risk. *Am. J. Psychiatry* **166**, 216–225 (2009).
- Amunts, K. et al. Cytoarchitectonic mapping of the human amygdala, hippocampal region and entorhinal cortex: intersubject variability and probability maps. *Anat. Embryol.* **210**, 343–352 (2005).
- Haramati, S. et al. MicroRNA as repressors of stress-induced anxiety: the case of amygdalar miR-34. *J. Neurosci.* **31**, 14191–14203 (2011).
- Dias, B. G. et al. Amygdala-dependent fear memory consolidation via miR-34a and Notch signaling. *Neuron* **83**, 906–918 (2014).
- Mier, D. et al. Evidence for altered amygdala activation in schizophrenia in an adaptive emotion recognition task. *Psychiatry Res.* **221**, 195–203 (2014).
- Pankow, A. et al. Altered amygdala activation in schizophrenia patients during emotion processing. *Schizophr. Res.* **150**, 101–106 (2013).
- Suslow, T. et al. Automatic amygdala response to facial expression in schizophrenia: initial hyperresponsivity followed by hyporesponsivity. *BMC Neurosci.* **14**, 140 (2013).
- Fromer, M. et al. Gene expression elucidates functional impact of polygenic risk for schizophrenia. *Nat. Neurosci.* **19**, 1442–1453 (2016).
- Wu, T. D. & Nacu, S. Fast and SNP-tolerant detection of complex variants and splicing in short reads. *Bioinformatics* **26**, 873–881 (2010).
- Li, H. et al. The sequence alignment/map format and SAMtools. *Bioinformatics* **25**, 2078–2079 (2009).
- Trapnell, C. et al. Differential analysis of gene regulation at transcript resolution with RNA-seq. *Nat. Biotechnol.* **31**, 46–53 (2013).
- Harrow, J. et al. GENCODE: the reference human genome annotation for The ENCODE Project. *Genome Res.* **22**, 1760–1774 (2012).
- Love, M. I., Huber, W. & Anders, S. Moderated estimation of fold change and dispersion for RNA-seq data with DESeq2. *Genome Biol.* **15**, 550 (2014).
- Chen, C., Khaleel, S. S., Huang, H. & Wu, C. H. Software for pre-processing Illumina next-generation sequencing short read sequences. *Source Code Biol. Med.* **9**, 8 (2014).
- Hach, F. et al. mrsFAST: a cache-oblivious algorithm for short-read mapping. *Nat. Methods* **7**, 576–577 (2010).
- Ripke, S. et al. Genome-wide association analysis identifies 13 new risk loci for schizophrenia. *Nat. Genet.* **45**, 1150–1159 (2013).
- Schizophrenia Working Group of the Psychiatric Genomics C. Biological insights from 108 schizophrenia-associated genetic loci. *Nature* **511**, 421–427 (2014).
- Fromer, M. et al. De novo mutations in schizophrenia implicate synaptic networks. *Nature* **506**, 179–184 (2014).
- Kim, A. H. et al. MicroRNA expression profiling in the prefrontal cortex of individuals affected with schizophrenia and bipolar disorders. *Schizophr. Res.* **124**, 183–191 (2010).
- Sun, X. Y. et al. A preliminary analysis of microRNA as potential clinical biomarker for schizophrenia. *Am. J. Med. Genet. B* **168**, 170–178 (2015).
- Lai, C. Y. et al. MicroRNA expression aberration as potential peripheral blood biomarkers for schizophrenia. *PLoS ONE* **6**, e21635 (2011).
- Balu, D. T. et al. Multiple risk pathways for schizophrenia converge in serine racemase knockout mice, a mouse model of NMDA receptor hypofunction. *Proc. Natl. Acad. Sci. USA* **110**, E2400–2409 (2013).
- Smalheiser, N. R. et al. MicroRNA expression is down-regulated and reorganized in prefrontal cortex of depressed suicide subjects. *PLoS ONE* **7**, e33201 (2012).

37. Shu, R. et al. *APP intracellular domain* acts as a transcriptional regulator of miR-663 suppressing neuronal differentiation. *Cell. Death Dis.* **6**, e1651 (2015).
38. Zhou, R. et al. Evidence for selective microRNAs and their effectors as common long-term targets for the actions of mood stabilizers. *Neuropsychopharmacology* **34**, 1395–1405 (2009).
39. Stefansson, H. et al. Common variants conferring risk of schizophrenia. *Nature* **460**, 744–747 (2009).
40. Goytain, A. & Quamme, G. A. Functional characterization of ACDP2 (ancient conserved domain protein), a divalent metal transporter. *Physiol. Genom.* **22**, 382–389 (2005).
41. Arjona, F. J. et al. CNNM2 mutations cause impaired brain development and seizures in patients with hypomagnesemia. *PLoS. Genet.* **10**, e1004267 (2014).
42. Ruano, D. et al. Association of the gene encoding neurogranin with schizophrenia in males. *J. Psychiatr. Res.* **42**, 125–133 (2008).
43. Ohi, K. et al. Influence of the NRG1 gene on intellectual ability in schizophrenia. *J. Hum. Genet.* **58**, 700–705 (2013).
44. Walton, E. et al. The impact of genome-wide supported schizophrenia risk variants in the neurogranin gene on brain structure and function. *PLoS. ONE* **8**, e76815 (2013).
45. Ohi, K. et al. Functional genetic variation at the NRG1 gene and schizophrenia: evidence from a gene-based case-control study and gene expression analysis. *Am. J. Med. Genet. B* **159B**, 405–413 (2012).
46. Ling, K. H. et al. Spatiotemporal regulation of multiple overlapping sense and novel natural antisense transcripts at the Nrgn and Camk2n1 gene loci during mouse cerebral corticogenesis. *Cereb. Cortex* **21**, 683–697 (2011).
47. Egan, M. F. et al. Variation in GRM3 affects cognition, prefrontal glutamate, and risk for schizophrenia. *Proc. Natl. Acad. Sci. USA* **101**, 12604–12609 (2004).
48. Mossner, R. et al. Further evidence for a functional role of the glutamate receptor gene GRM3 in schizophrenia. *Eur. Neuropsychopharmacol.* **18**, 768–772 (2008).
49. Allen, N. C. et al. Systematic meta-analyses and field synopsis of genetic association studies in schizophrenia: the SzGene database. *Nat. Genet.* **40**, 827–834 (2008).
50. Knable, M. B. & Weinberger, D. R. Dopamine, the prefrontal cortex and schizophrenia. *J. Psychopharmacol.* **11**, 123–131 (1997).
51. Wible, C. G. et al. Prefrontal cortex, negative symptoms, and schizophrenia: an MRI study. *Psychiatry Res.* **108**, 65–78 (2001).
52. Schizophrenia Psychiatric Genome-Wide Association Study C. Genome-wide association study identifies five new schizophrenia loci. *Nat. Genet.* **43**, 969–976 (2011).
53. Silber, J. et al. miR-124 and miR-137 inhibit proliferation of glioblastoma multiforme cells and induce differentiation of brain tumor stem cells. *BMC Med.* **6**, 14 (2008).
54. Xu, Y. et al. MicroRNAs and target site screening reveals a pre-microRNA-30e variant associated with schizophrenia. *Schizophr. Res.* **119**, 219–227 (2010).
55. Han, J. et al. Functional implications of miR-19 in the migration of newborn neurons in the adult brain. *Neuron* **91**, 79–89 (2016).
56. Murai, K. et al. The TLX-miR-219 cascade regulates neural stem cell proliferation in neurodevelopment and schizophrenia iPSC model. *Nat. Commun.* **7**, 10965 (2016).
57. Topol, A. et al. Dysregulation of miRNA-9 in a subset of schizophrenia patient-derived neural progenitor cells. *Cell. Rep.* **15**, 1024–1036 (2016).